

- Staros, J. V., Morgan, D. G., & Appling, D. R. (1981) *J. Biol. Chem.* 256, 5890-5893.  
 Steck, T. L. (1978) *J. Supramol. Struct.* 8, 311-324.  
 Tilney, L. G., & Detmers, P. (1975) *J. Cell Biol.* 66, 508-520.  
 Wang, K., & Richards, F. M. (1974a) *Isr. J. Chem.* 12, 375-389.

- Wang, K., & Richards, F. M. (1974b) *J. Biol. Chem.* 249, 8005-8018.  
 Wang, K., & Richards, F. M. (1975) *J. Biol. Chem.* 250, 6622-6626.  
 Wofsy, L., & Singer, S. J. (1963) *Biochemistry* 2, 104-116.  
 Wold, F. (1972) *Methods Enzymol.* 25, 623-651.

## Orthogonal Packing of $\beta$ -Pleated Sheets in Proteins<sup>†</sup>

Cyrus Chothia\* and Joël Janin\*

**ABSTRACT:** Two classes of  $\beta$ -sheet to  $\beta$ -sheet packing can be distinguished in globular proteins. Both classes have  $\beta$  sheets with the usual right-handed twist packed face to face. In *orthogonal  $\beta$ -sheet packings*, the strand directions of the different  $\beta$  sheets are 90° to each other. Twisted  $\beta$  sheets in this orientation have anticomplementary surfaces: one pair of diagonally opposite corners in the  $\beta$  sheets is very close, and the other pairs of corners splay apart. At the close corners, the  $\beta$  sheets are usually covalently connected: a strand that is part of one  $\beta$  sheet turns through a right-handed bend to become part of the second  $\beta$  sheet. The bend may occur at a  $\beta$  bulge, or over a stretch of residues with a characteristic conformation, forming what we call a  $\beta$  bend. Contacts between the  $\beta$  sheets occur along the diagonal joining the close

corners. They involve about one-fourth of the  $\beta$ -sheet residues, and two-thirds of them are Val, Ile, or Leu. Elsewhere, the space between the  $\beta$  sheets is filled by side chains from other parts of the protein, often  $\alpha$  helices placed at the splayed corners. Examples of orthogonal  $\beta$ -sheet packing are found in alcohol dehydrogenase, the acid proteases, the trypsin family, papain, staphylococcal nuclease, and thermolysin. In *aligned  $\beta$ -sheet packings*, the angle between the strand directions of the packed  $\beta$  sheets is  $\sim 30^\circ$ . In this orientation, the twisted  $\beta$ -sheet surfaces are complementary. The principles governing this class of  $\beta$ -sheet packings have been described previously. Here we discuss the differences and similarities of the aligned and orthogonal packing classes.

In proteins, the polypeptide chain folds into  $\alpha$  helices and  $\beta$ -pleated sheets, which close-pack to form the three-dimensional structure. It has been shown that, underlying the great variety of protein structures, there are *general principles* that govern how  $\alpha$  helices pack onto other  $\alpha$  helices and onto  $\beta$ -pleated sheets (Crick, 1953; Chothia et al., 1977, 1981; Richmond & Richards, 1978; Efimov, 1977, 1979; Cohen et al., 1980, 1981; Janin & Chothia, 1980). We discuss here the principles that govern the packing together of  $\beta$ -pleated sheets.

Proteins whose secondary structure consists mostly of  $\beta$ -pleated sheets have a number of common features. They are layer structures, usually bilayers or "sandwiches". Each layer is a  $\beta$  sheet with a right-handed twist and forms face to face contacts with other layers (Figure 1). The relative orientation of the  $\beta$  sheets in contact defines two classes of structures (Chothia et al., 1977). In one class, the mean direction of the  $\beta$  strands in one layer is at a small angle (about  $\sim 30^\circ$ ) to that of the  $\beta$  strands in the other layer. An example of this class is prealbumin. In the second class, this angle is close to 90°. The packing of the  $\beta$  sheets in the first class will be referred to as *aligned  $\beta$ -sheet packing*, as opposed to the *orthogonal  $\beta$ -sheet packing* of the second class.

Detailed descriptions of aligned  $\beta$ -sheet packings have been published (Cohen et al., 1981; Chothia & Janin, 1981), and most of this paper will be devoted to an analysis of orthogonal

$\beta$ -sheet packings. We present a general model and compare it to what is actually observed in proteins that contain orthogonally packed  $\beta$  sheets. In addition, we define a peculiar conformation of the polypeptide chain, the  $\beta$  bend, which enables  $\beta$  strands to bend by 90° without disturbing their H-bond pattern.

### Experimental Procedures

We have used computer graphics and numerical calculations to examine in detail the conformation and packing of the  $\beta$ -pleated sheets in five proteins whose structures have been determined by X-ray analysis: alcohol dehydrogenase, catalytic domain (Eklund et al., 1976); elastase, first domain (Sawyer et al., 1978); papain, second domain (Drenth et al., 1971); penicillopepsin, first domain (Hsu et al., 1977); staphylococcal nuclease (Arnold et al., 1971).

Elastase and penicillopepsin are taken as representatives of two large families of homologous structures: elastase for trypsin-like serine proteases and penicillopepsin for acid proteases. Residue numbering for elastase is based on its alignment with chymotrypsin and that for penicillopepsin on its alignment with pig pepsin.

A general model for orthogonal  $\beta$ -sheet packing is presented in Figure 2. This model will be useful in understanding the relation and coherence of the rather complex structural descriptions given in the next section. The major features of the model are the following:

(a) The  $\beta$ -pleated sheets are placed face to face with the strand directions, making a right angle. *Two of the strands, labeled a and d, form part of both  $\beta$  sheets* and join them covalently at two diagonally opposite corners. Each  $\beta$  sheet has the normal twist. [This twist is right-handed when the  $\beta$  sheet is viewed from an end, as for the top  $\beta$  sheet of Figure

<sup>†</sup> From William Ramsay, Ralph Foster and Christopher Ingold Laboratories, University College London, London WC1E 6BT, England, the M.R.C. Laboratory of Molecular Biology, Cambridge CB2 2QH, England (C.C.), and the Laboratoire de Biologie Physicochimique, Université Paris-Sud, 91405 Orsay, France (J.J.). Received October 9, 1981; revised manuscript received March 12, 1982. This work was supported by the Royal Society and the U.S. National Institute of General Medical Sciences (1-RO1-GM25434).

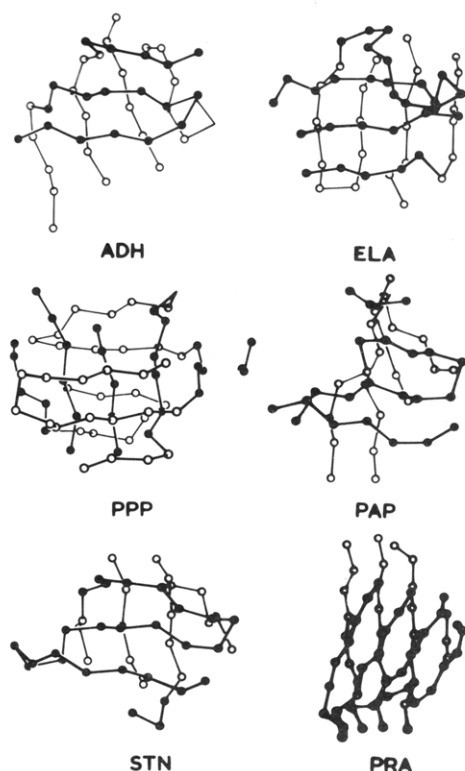


FIGURE 1: Arrangement of the packed  $\beta$  sheets in alcohol dehydrogenase (ADH), elastase (ELA), penicillopepsin (PPP), papain (PAP), staphylococcal nuclease (STN), and prealbumin (PRA). The circles represent the position of  $C_\alpha$  atoms. Except for penicillopepsin, the open circles represent the far  $\beta$  sheets and the closed circles the near  $\beta$  sheets. Penicillopepsin has three  $\beta$  sheets that form a trilayer structure, and here the middle  $\beta$  sheet is represented by closed circles and far and near  $\beta$  sheets are represented by open circles. The angle between the direction of the strands of the packed sheets is near  $90^\circ$  except for prealbumin, shown here as an example of aligned packing where it is  $-30^\circ$ . (The negative sign denotes the clockwise rotation of the near  $\beta$  sheet relative to the far  $\beta$  sheet.)

2b, and left-handed when it is viewed from an edge, as for the bottom  $\beta$  sheet of the same figure (Chothia, 1973).]

Due to their twist, the two  $\beta$  sheets are only in contact near the diagonal joining the two covalently linked corners—the *close corners*. At the other two corners, the  $\beta$  sheets splay apart.

(b) The strands that covalently link the two  $\beta$  sheets at the close corners have *right-handed*  $90^\circ$  bends. Strands a and d in Figure 2 form H bonds with  $\beta$  strands of both top and bottom  $\beta$  sheets. They bend through  $90^\circ$  when passing from one  $\beta$  sheet to the other. Figure 3 describes the right-handed bends in strands a and d; for comparison, it also shows strands with left-handed bends. The hand of the bend forming connections at the close corners is the same as the hand of the twist in the  $\beta$  sheet. Left-handed bends could occur only at corners where the two layers of the  $\beta$  sandwich splay apart (compare Figures 2 and 3).

The bend in the strands can be produced by the insertion of a residue in an  $\alpha_R$  conformation to form a "classic  $\beta$  bulge" (Richardson et al., 1978), or by the strand being strongly twisted to form that we call a " $\beta$  bend", which we shall describe below.

(c) The packing of the  $\beta$  sheets involves contacts between side chains. The spacing between residues pointing inside is larger along the strands (where the  $C_\alpha$ 's of residues  $i$  and  $i + 2$  are separated by about  $7.0 \text{ \AA}$ ) than between strands (the  $C_\alpha$ 's of residues in adjacent  $\beta$  strands are about  $4.5 \text{ \AA}$  apart). Thus, there cannot be a *regular* pattern of intercalating side

Table I:  $\Omega$  Angles in Orthogonal  $\beta$ -Sheet Packings<sup>a</sup>

protein	$\Omega$ (deg)	strands used in	
		$\beta$ sheet I	$\beta$ sheet II
alcohol dehydrogenase	77	34–39, 149–154	68–72, 88–92
elastase	96	31–36, 64–68	50–54, 103–108
papain	83	130–134	169–174
penicillopepsin I	79	38–42, 119–123	71–75, 79–83
penicillopepsin II	71	21–24, 88–93	38–42, 119–123
staphylococcal nuclease	79	21–26, 31–36	71–75, 91–95

<sup>a</sup>  $\Omega$  is the angle between the mean strand directions when projected onto the plane of  $\beta$ -sheet to  $\beta$ -sheet contact.  $C_\alpha$  atoms of the residues listed in this table are used for fitting vectors to the central  $\beta$  strands of each  $\beta$  sheet. The mean strand directions are derived from these vectors. Positive values of  $\Omega$  indicate right-handed screw rotations from one layer to the other.

chains, as is found in contacts between  $\alpha$  helices (Chothia et al., 1977, 1981; Efimov, 1977, 1979; Richmond & Richards, 1978). The surfaces forming  $\beta$ -sheet to  $\beta$ -sheet contacts tend to be smooth and hydrophobic and favor Val, Ile, and Leu residues. At the corner where the  $\beta$  sheets splay apart, the space can be filled by an  $\alpha$  helix or other parts of the protein structure.

(d) If we straighten one bent strand and break the other to unfold the packing, we obtain the H-bond pattern of Figure 2c, where the two  $\beta$  sheets appear to constitute a single  $\beta$  sheet with *staggered strands*.

## Results

**Relative Orientation and Twist of the  $\beta$  Sheets.** Figure 1 shows that the five proteins contain  $\beta$ -pleated sheets packed face to face. Penicillopepsin has three such  $\beta$  sheets, forming a three-layered structure. The four other proteins have only two layers. The relative orientation of the packed  $\beta$  sheets can be defined by the angle  $\Omega$ —the angle between the mean strand directions when projected onto their plane of contact.  $\Omega$  values were calculated from the atomic coordinates of the proteins and are presented in Table I. The six values have a mean of  $81^\circ$ , standard deviation  $8^\circ$ . For aligned  $\beta$ -sheet packings, e.g., prealbumin (Figure 1),  $\Omega$  values are in the range of  $-30^\circ \pm 15^\circ$  (Chothia & Janin, 1981).

The twist of the  $\beta$  sheet can be expressed in terms of the dihedral angle between pairs of adjacent strands. Figure 4 is a histogram of the angles between the 33 pairs of adjacent strands in the five proteins. The mean value is  $-24^\circ$ , and its standard deviation is  $17^\circ$ . For the  $\beta$  sheets in  $\alpha/\beta$  proteins, the dihedral angle between strands has a mean of  $-19^\circ$ , standard deviation  $7^\circ$ , and for  $\beta$  sheets involved in aligned packings, the value is  $-17^\circ$ , standard deviation  $7^\circ$  (Janin & Chothia, 1980; Chothia & Janin, 1981). Thus, the twist of the  $\beta$  sheets found in orthogonal packings has a wider variation and somewhat higher mean value than that which is found for  $\beta$  sheets in other types of packing.

**Folding of the  $\beta$  Sheets in the Five Proteins.** Figure 5 shows H-bond diagrams for the  $\beta$  sheets in the five proteins. In this figure, single  $\beta$  sheets have been made from two (or three in penicillopepsin) by straightening and, when necessary, cleaving  $\beta$  strands joining the top and bottom layers of the  $\beta$  sandwiches. Letters A, B, C, and D mark the points where the strands are bent and cross from one layer to the other. At these points, not only do the  $\beta$  strands deviate from a straight line but also they change their H-bonding partners. These positions are marked by letters on the model in Figure 2 where they correspond to the close corners.

The first domain of *elastase* forms a six-stranded antiparallel  $\beta$  sheet (Figure 5a), which folds into two layers connected by

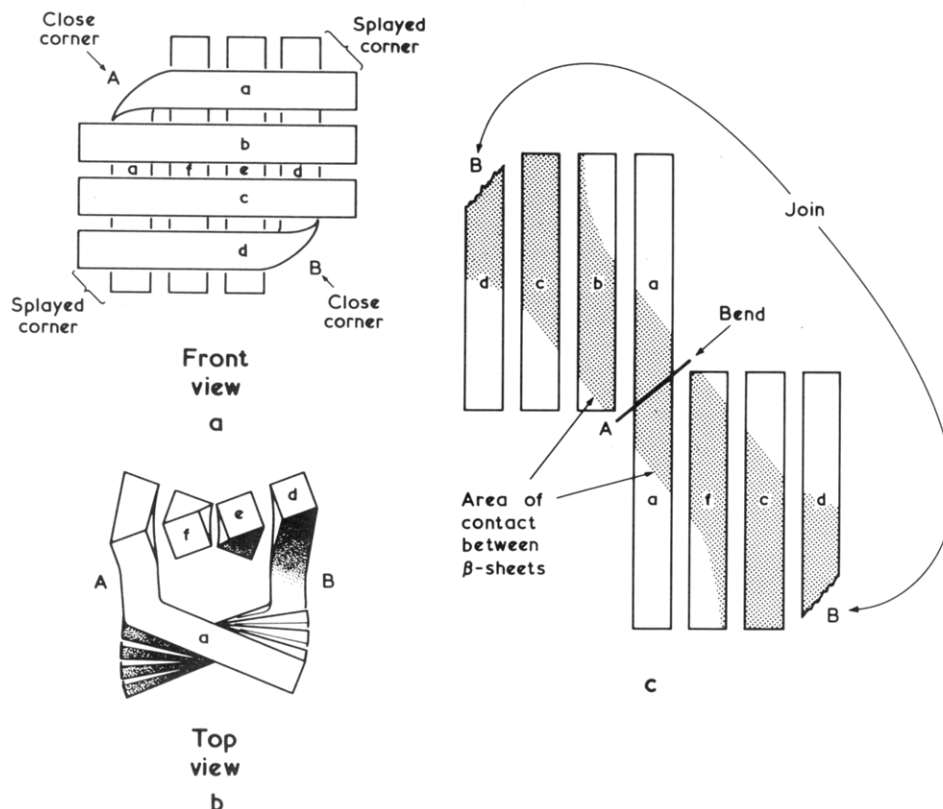


FIGURE 2: Model for the orthogonal packing of  $\beta$  sheets. The strands are represented by rods with square cross section. The  $\beta$  sheets have the normal right-handed twist, and when placed face to face with their strands orthogonal, they have two corners that come close to the other  $\beta$  sheet (A and B) and two that splay away. Here the strands at the close corners are joined, so a and d belong to both the near and far  $\beta$  sheets. The joins are formed by right-handed bends (see Figure 3). If the packing is opened out by straightening bend A and breaking the chain at B, we get a single  $\beta$  sheet with staggered strands (Figure 2c).

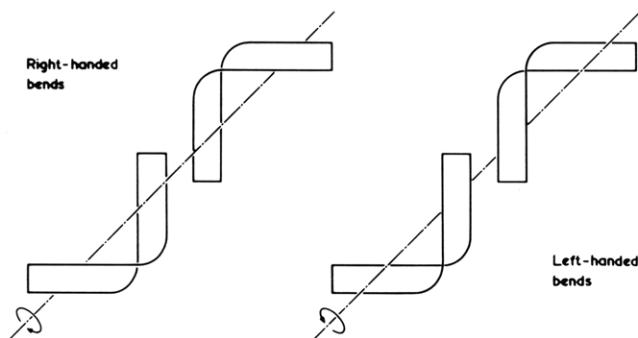


FIGURE 3: Right- and left-handed bends. The handedness of the bends is given by the direction of their rotation about an imaginary axis.

$\beta$  strands 36D-49 and 81-91. Strand 36D-49 bends by about  $90^\circ$  at point A, and strand 81-91 at point B, opposite to A on the diagonal joining close corners, in accordance with the model shown in Figure 2. At point B, residue Gln-86 has an  $\alpha_R$  conformation, and the polypeptide chains form a classic  $\beta$  bulge as defined by Richardson et al. (1978). Residue Gln-86 is shown bulging out of the alignment in the H-bond diagram on Figure 5a. The bend created by the  $\beta$  bulge is right-handed. At point A, the polypeptide chain also takes a right-handed  $90^\circ$  turn, yet it remains in  $\beta$ -like conformation. This is what we call a  $\beta$  bend and describe in detail in the next section. The particular  $\beta$  bend in strand 36D-49 is between two classic  $\beta$  bulges at Thr-41 and Ile-47.

The major part of the catalytic domain of *alcohol dehydrogenase* is formed by a large  $\beta$  sheet folded on itself. It has five antiparallel strands (Figure 5b). Strands 34-45, 68-77, and 148-160 join the two layers. The bends at A1 on strand 34-45 and at A2 on strand 68-77 are classic  $\beta$  bulges

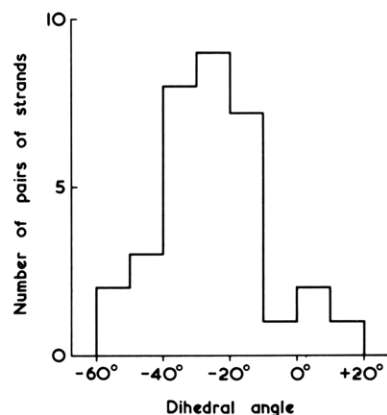


FIGURE 4: Histogram of the dihedral angles between adjacent strands in the  $\beta$  sheets of five proteins (see Figure 5).

and form one close corner. The connection between strands 148-154 and 156-160 forms the other close corner (point B). At point B, residues 154-156 have a helical conformation, so that the polypeptide chain turns by about  $270^\circ$  through an incomplete turn of helix, instead of turning by one-fourth of a turn as in a  $\beta$  bulge. The bend is still right-handed.

Residues 1-99 of *staphylococcal nuclease* form a six-stranded antiparallel  $\beta$  sheet folded orthogonally on itself (Figure 5c). Top and bottom are joined by  $\beta$  bends at points A and B.

The first domain of *penicillopepsin* is a three-layer orthogonal  $\beta$  packing (Figures 1 and 5d). The top  $\beta$  sheet fuses to the middle  $\beta$  sheet at points D1, D2, and C, which form close corners at opposite ends of a diagonal. The bottom and middle  $\beta$  sheets fuse at only one close corner, corresponding

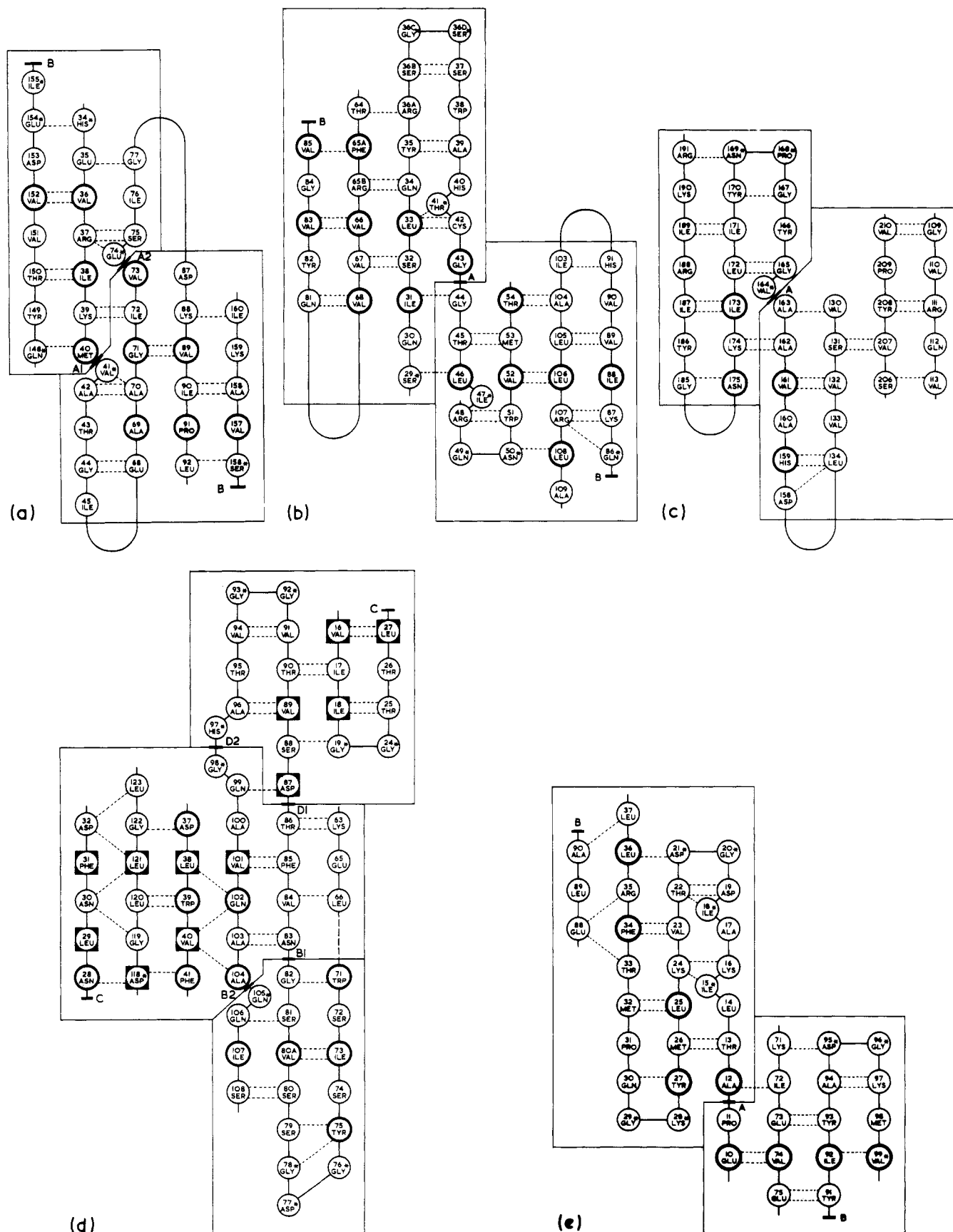


FIGURE 5: Plans showing the residues and hydrogen bonds that form the five orthogonal  $\beta$ -sheet packings. Dotted lines indicate hydrogen bonds. Residues marked with an asterisk have  $\phi, \psi$  values outside the  $\beta$  region. Residues surrounded by thick circles form the  $\beta$ -sheet to  $\beta$ -sheet contacts. The separate  $\beta$  sheets are boxed by a thin continuous line. The orthogonal packing involves bending the strands at the point labeled A (or A1 and A2) and joining them at B (see the model in Figure 2). The figures are drawn so that except for penicillopepsin the near  $\beta$  sheet on the top left folds forward over the far  $\beta$  sheet on the bottom right. Note the diagonal pattern formed by contact residues and the staggered pattern formed by the strands. (a) Alcohol dehydrogenase; (b) elastase; (c) papain; (d) penicillopepsin; in this figure, the near  $\beta$  sheet is on the bottom right and folds *forward* at B1 and B2; the far  $\beta$  sheet is on the top right and folds *backward* at D1 and D2 and joins at C; both faces of the middle  $\beta$  sheet are covered; residues surrounded by thick circles form front to middle  $\beta$ -sheet contacts, and those in squares form middle to back  $\beta$ -sheet contacts; (e) staphylococcal nuclease.

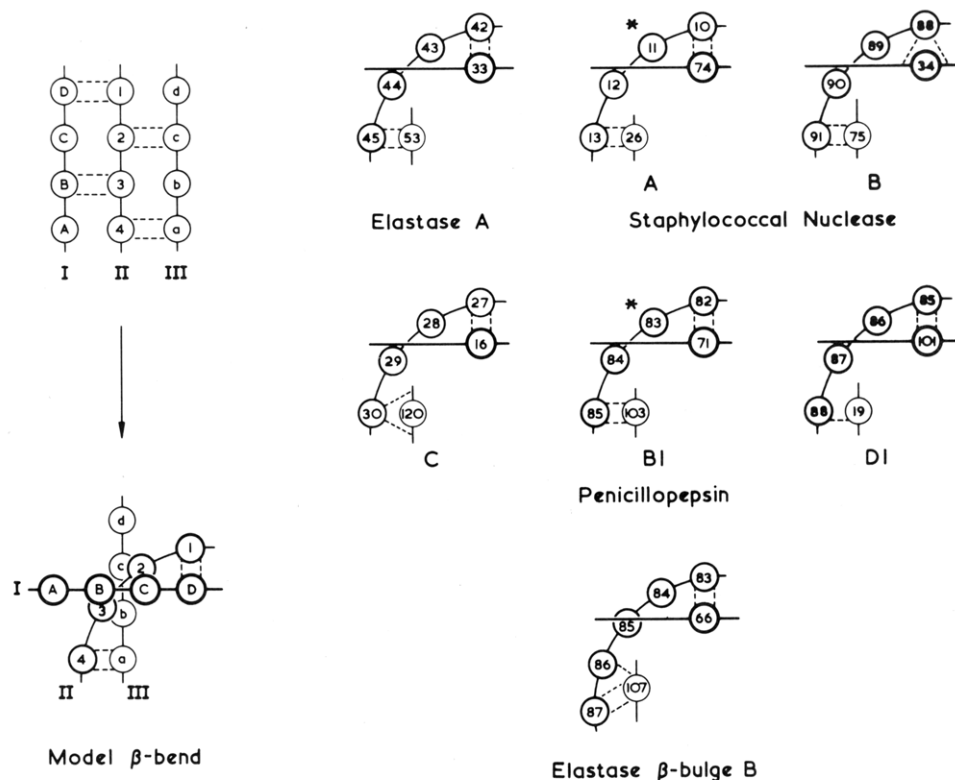


FIGURE 6:  $\beta$  bends in four proteins. A model with three  $\beta$  strands is presented on the left. They form an antiparallel  $\beta$  sheet (top left) to which a strong right-handed twist is applied (bottom left), such that strands I and III now form a right angle. H bonds are maintained. The side chains of residues labeled b, 3, and B now pack against each other. Schematic descriptions of  $\beta$  bends in elastase, staphylococcal nuclease, penicillopepsin, and triosephosphate isomerase may be compared to the model. The  $\beta$  bulge at Gln-86 in elastase is represented with the same convention to show its similarity to  $\beta$  bends; strand II has five residues instead of four in the bends. Residues labeled with an asterisk have polyproline II conformations (Table II); Gln-86 in elastase has an  $\alpha_R$  conformation ( $\phi = -85^\circ$ ,  $\psi = -23^\circ$ ). The nomenclature of  $\beta$  bends is described in Figure 5.

to points B1 and B2. At point B2, there is a classic  $\beta$  bulge, and at points B1, C, and D1, there are  $\beta$  bends. The middle and bottom layers also fuse at point D2 where there is a two-residue connection (His-97-Gly-98) between strands 93-96 and 99-108; as in alcohol dehydrogenase, the connection is through an incomplete turn of a right-handed helix.

The C-terminal domain of *papain* (Figure 5e) is similar to staphylococcal nuclease and elastase in having a six-stranded antiparallel  $\beta$  sheet folded on itself. But in this structure there is only a single close corner formed by the classic  $\beta$  bulge at point A.

**Conformation of the Strands at the Close Corners:  $\beta$  Bends and  $\beta$  Bulges.** We have just seen cases of  $\beta$  strands that bend through a right angle rather than being straight as usual. The bend takes place over a few residues which have  $\beta$  (or  $\beta$ -like) conformations; that is, their  $\phi$ ,  $\psi$  dihedral angles are in the top left quadrant of the Ramachandran diagram (Table II). We call such structures  $\beta$  bends, not to be confused with  $\beta$  turns (Venkatachalam, 1968), in which the polypeptide chain turns by  $180^\circ$  rather than  $90^\circ$ .  $\beta$  bends are found in elastase, staphylococcal nuclease, and penicillopepsin, but also in other proteins (in triosephosphate isomerase, for instance).

A schematic representation of a  $\beta$  bend has three  $\beta$  strands, I, II, and III (Figure 6). Strands I and III are straight. They point in orthogonal directions with their side chains facing each other. Strand II in between has its residue 1 forming H bonds with strand I and residue 4 forming H bonds with strand III. If strand I had no twist, the peptide groups of residues 1 and 4 would point in opposite directions, but the twist is so strong here that these peptide groups are at  $90^\circ$  instead of  $180^\circ$  and may H bond to two orthogonal  $\beta$  strands. Thus,  $\beta$  bends are characterized by a very strong right-handed twist occurring

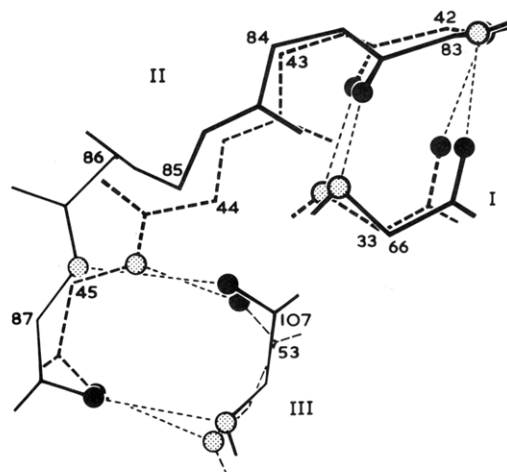


FIGURE 7: Comparison of  $\beta$  bends and  $\beta$  bulges. The  $\beta$  bulge forming a close corner at point B in elastase (Figure 5a) is superimposed onto the  $\beta$  bend at point A in the same protein. The superposition is done by a least-squares fit of the main-chain atoms of the two end residues in strand II and one end residue from each of strands I and II (see Figure 6); i.e., residues 33, 42, 45, and 53 are superimposed on 66, 83, 87, and 107. The root mean square distance between equivalent atoms is 0.9 Å.

over three peptide units in the middle  $\beta$  strand, II. This applies to antiparallel  $\beta$  strands and, with little modification, to the parallel  $\beta$  strands of penicillopepsin.

A convenient description of the twist of  $\beta$  strands simply uses the  $\phi$ ,  $\psi$  dihedral angles. Nontwisted  $\beta$  strands correspond to points close to one diagonal (the  $\phi + \psi = 0$  diagonal) of the Ramachandran diagram, right-handed twists to points on the right ( $\phi + \psi > 0$ ), and left-handed twists to points on the

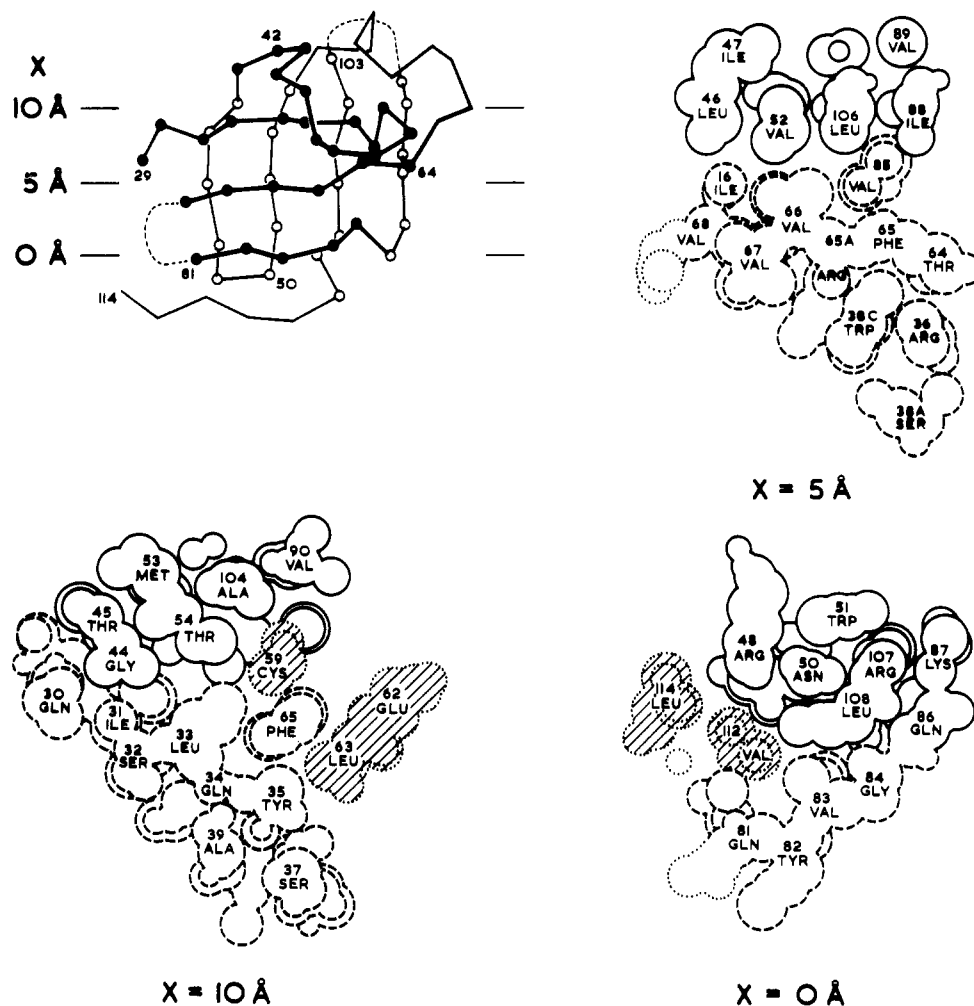


FIGURE 8: Residue packing at the  $\beta$ -sheet interface in domain 1 of elastase. This figure shows sections cut out through a computer-generated space-filling model of the protein. The position of the section is indicated on a drawing of the  $C_\alpha$  atoms where the  $\beta$ -sheet residues are indicated by open or closed circles. The sections are cut perpendicular to the  $\beta$ -sheet interface with the strands in the near  $\beta$  sheet in the plane of the page, and indicated by broken lines, and the strands of the far  $\beta$  sheet perpendicular to the page, and indicated by solid lines. Residues not in a  $\beta$  sheet are shaded. Each space-filling drawing consists of three sections cut at 1-Å separation and superimposed so that they describe a 2-Å-thick slice.

left ( $\phi + \psi < 0$ ) of the diagonal. The center of the permitted region of the  $\phi, \psi$  space corresponding to extended chain conformations and the center of the actual distribution of  $\phi, \psi$  angles in  $\beta$  sheets are to the right of the diagonal. Alternative interpretations of the twist have been proposed (Weatherford & Salemme, 1979). They assume systematic deviations from the standard geometry of peptide units in  $\beta$  sheets. Whether this is correct or not, the  $\phi, \psi$  angles with a standard geometry are sufficient for our present purpose: in the  $\beta$  region, positive values of  $\phi + \psi$  indicate a right-handed twist. Table II shows that the average value of  $\phi + \psi$  in the 24 peptide units forming six  $\beta$  bends is high ( $27^\circ$  instead of an average of  $15^\circ$  in the remainder of the  $\beta$  sheets in the four proteins quoted).

The high average value may result from several peptide units in strand II having large  $\phi + \psi$  values: the rotation of the chain is spread over two or three residues. In four cases, however (Gly-43 in elastase, Asn-83 and Asp-87 in penicillopepsin, and Pro-11 in staphylococcal nuclease), the rotation of the chain is localized on a single residue with  $\phi + \psi = 67-90^\circ$ , placed at position 2 or 3 in the  $\beta$  bend. (Note that positions 2 and 3, and also 1 and 4, are equivalent, due to the symmetry operation that exchanges strands I and III.) In these four cases, the conformation of the residue at the bend approaches that of polyproline II, hence the positive rotation of

the chain by about one-fourth of the turn (one-third in polyproline). Another way of creating a positive rotation of similar amplitude is the insertion of a residue in the  $\alpha_R$  conformation. In a  $\beta$  sheet, this creates a classic  $\beta$  bulge. It can be seen in Figure 4 of Richardson et al. (1978) that classic  $\beta$  bulges do form right-handed bends in the  $\beta$  strand where the  $\alpha_R$  residue occurs. The actual effect of the  $\beta$  bulge on the chain direction depends on the conformation of adjacent residues. Figure 7 of this paper shows the classic  $\beta$  bulge at Gln-86 in elastase superimposed onto the  $\beta$  bend at Gly-43. The two are very similar, except for the insertion of one residue in the  $\beta$  bulge.

**$\beta$ -Sheet to  $\beta$ -Sheet Packing.** The residues that form the  $\beta$ -sheet to  $\beta$ -sheet contacts are indicated on the H-bond diagrams (Figure 5) by thick circles or square boxes. To analyze and illustrate the packing of these residues, we cut serial sections through space-filling models generated from atomic coordinates. A selection of computer-drawn sections appears in Figures 8-11 for the orthogonal  $\beta$  packings studied here. The cleavage plane is perpendicular to the mean plane of the  $\beta$ -sheet to  $\beta$ -sheet interface. Its position is shown on chain tracing diagrams. The orientation in all of the sections shown is such that the strands of the near  $\beta$  sheet run in the plane of the page, while  $\beta$  strands of the far  $\beta$  sheet are perpendicular to the page. "Near" and "far" refer to the position of  $\beta$  sheets in the chain tracing diagrams.

Table II: Dihedral Angles (deg) in  $\beta$  Bends<sup>a</sup>

protein	residue	$\phi$	$\psi$	$\phi + \psi$
elastase bend A	Cys-42	-156	170	14
	Gly-43	-93	177	84
	Gly-44	-177	171	-6
	Thr-45	-135	114	-21
penicillopepsin bend C	Leu-27	-132	137	5
	Asn-28	-94	102	8
	Leu-29	-104	145	41
	Asn-30	-79	133	54
bend B1	Gly-42	-190	192	2
	Asn-83	-85	174	89
	Val-84	-108	123	15
	Phe-85	-128	144	16
bend D1	Phe-85	-128	144	16
	Thr-86	-111	124	13
	Asp-87	-136	203	67
	Ser-88	-117	120	3
staphylococcal nuclease bend A	Glu-10	-113	120	7
	Pro-11	-37	126	89
	Ala-12	-144	160	16
	Thr-13	-121	143	22
bend B	Gly-88	-68	122	54
	Leu-89	-76	84	8
	Ala-90	-151	169	18
	Tyr-91	-91	128	37

<sup>a</sup> Residues in strand II of six  $\beta$  bends (Figure 6). In each bend, the first and fourth residues are H bonded to  $\beta$  strands I and III, respectively.

(A) *Elastase*. The arrangement of the  $\beta$ -sheet residues in the orthogonal packing in the first domain of elastase is illustrated in Figure 8. Three sections through the orthogonal packing are shown. The front section slices through strand 31–36B, the middle section through strand 64–68, and the back section through strand 81–86. In the middle section, the two  $\beta$  sheets make contacts all along their interface. The side chains of residues Ile-31, Val-66, and Val-85 in the near  $\beta$  sheet are in contact with side chains of residues belonging to each of the four strands of the far  $\beta$  sheet: Ile-88, Leu-106, Val-52, and Leu-46. The situation is different in the front and back sections, which show the  $\beta$  sheets forming a wedge open either to the left or to the right. Because of the twist, the near  $\beta$  sheet, viewed here from an edge, rotates counterclockwise by  $\sim 60^\circ$  going from front to back, while the far  $\beta$  sheet, viewed from an end, rotates clockwise. Thus, contacts between residues of the two  $\beta$  sheets occur only to the left of the front section and to the right of the back section. As a consequence, the pattern of contact residues (thick circles on the H-bond diagram of Figure 5a) shows not only their usual alternation along each  $\beta$  strand but also their clustering along a diagonal, in agreement with the model of Figure 2.

The opening of the wedge in the front and back sections corresponds to the splayed corners of the model. In elastase, they are filled with non- $\beta$ -sheet residues (shaded on the space-filling drawings): Val-59 and Leu-63 from the short helix 58–63 in the front section, Val-112 from a loop in the back of the structure.

(B) *Staphylococcal Nuclease and Alcohol Dehydrogenase*. The arrangement of the  $\beta$  sheets and their adjacent residues in the orthogonal  $\beta$  packings in these proteins is illustrated in Figure 9. The residues that form the  $\beta$ -sheet to  $\beta$ -sheet contacts (thick circles on Figures 5b and 5c) are near the diagonal joining the close corners. In staphylococcal nuclease, one splayed corner is filled by residues from the  $\alpha$  helix 59–69,

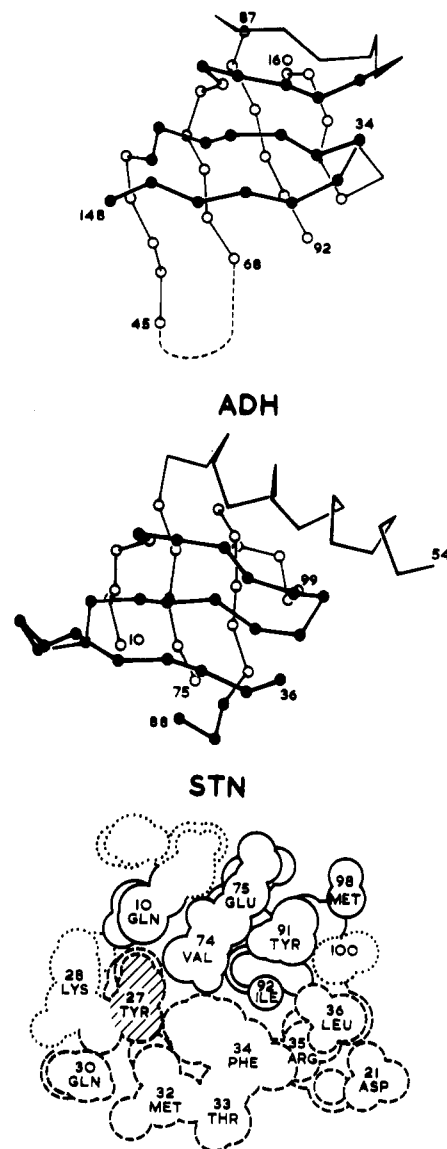


FIGURE 9: Orthogonal  $\beta$ -sheet packings in staphylococcal nuclease (STN) and alcohol dehydrogenase (ADH). In the drawings of the  $C_\alpha$  atoms,  $\beta$ -sheet residues are shown as open or filled circles. The space-filling drawing shows the packing in staphylococcal nuclease. Strand 30–36 in the near  $\beta$  sheet (broken lines) splay away from the far  $\beta$  sheet (solid lines), and Tyr-27 (shaded) fills the space between them (see text).

and in alcohol dehydrogenase, one splayed corner is filled by residues from the connecting loop 79–86. This is like elastase. At other splayed corners, the gap between the two layers is filled by a large side chain of a residue from a central  $\beta$  strand: Tyr-27 (dotted on Figure 9) in staphylococcal nuclease, Met-40 in alcohol dehydrogenase.

(C) *Penicillopepsin*. Four sections cut through the orthogonal  $\beta$  packing of the first domain of penicillopepsin are shown in Figure 10. The middle  $\beta$  sheet, with its  $\beta$  strands perpendicular to the figure, is sandwiched between the far  $\beta$  sheet (here, residues 16–27 and 87–96) and the near  $\beta$  sheet (residues 71–82 and 105–108), both sliced along their  $\beta$  strands.

The packing and the pattern of contacts formed by the far and middle  $\beta$  sheets, or by the middle and near  $\beta$  sheets, are the same as in the model and in elastase. The central  $\beta$  strand 71–76 of the near  $\beta$  sheet lies flat on the middle  $\beta$  sheet. The other two  $\beta$  strands splay away, and the space between the  $\beta$  sheets is filled by side chains from the short connecting helix

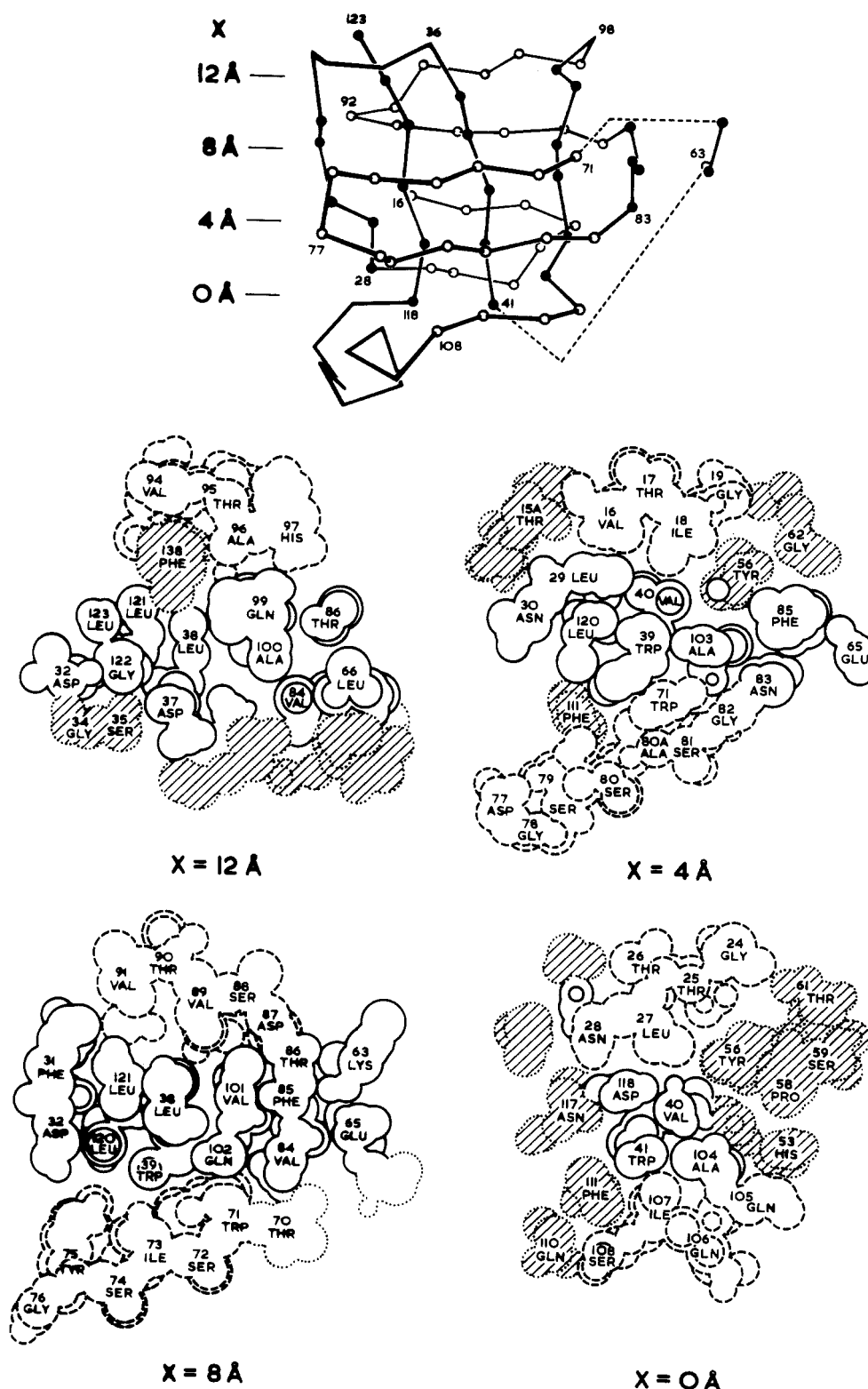


FIGURE 10: Residue packing at the  $\beta$ -sheet interface in domain 1 of penicillopepsin. See the legend to Figure 8 for a description of the convention used. This figure differs in that we have three rather than two  $\beta$  sheets. The far and near  $\beta$  sheets (broken lines) have their strands in the plane of the page; the middle  $\beta$  sheet (solid lines) has its strands perpendicular.

109–114. In the far  $\beta$  sheet, the two central strands 16–19 and 87–92 lie close to the middle  $\beta$  sheet while the two side strands splay away, 93–97 opening to the left and 24–27 opening to the right. The gaps between far and near  $\beta$  sheets are filled by side chains from the connecting loop 53–62 and from the  $\alpha$  helix 137–143.

Residues forming the far to middle  $\beta$ -sheet contact (in square boxes on Figure 5d), or the near to middle  $\beta$ -sheet

contact (thick circles), are clustered along the diagonals of the  $\beta$  sheets.

(D) *Papain*. Sections cut through the second domain of papain are shown in Figure 11. The  $\beta$  sheets are orthogonal and in contact about the close corner where they are joined by a classic  $\beta$  bulge in strand 158–168. These features are similar to those found in the other proteins and the model. However, in papain, the contact is restricted to only one corner,



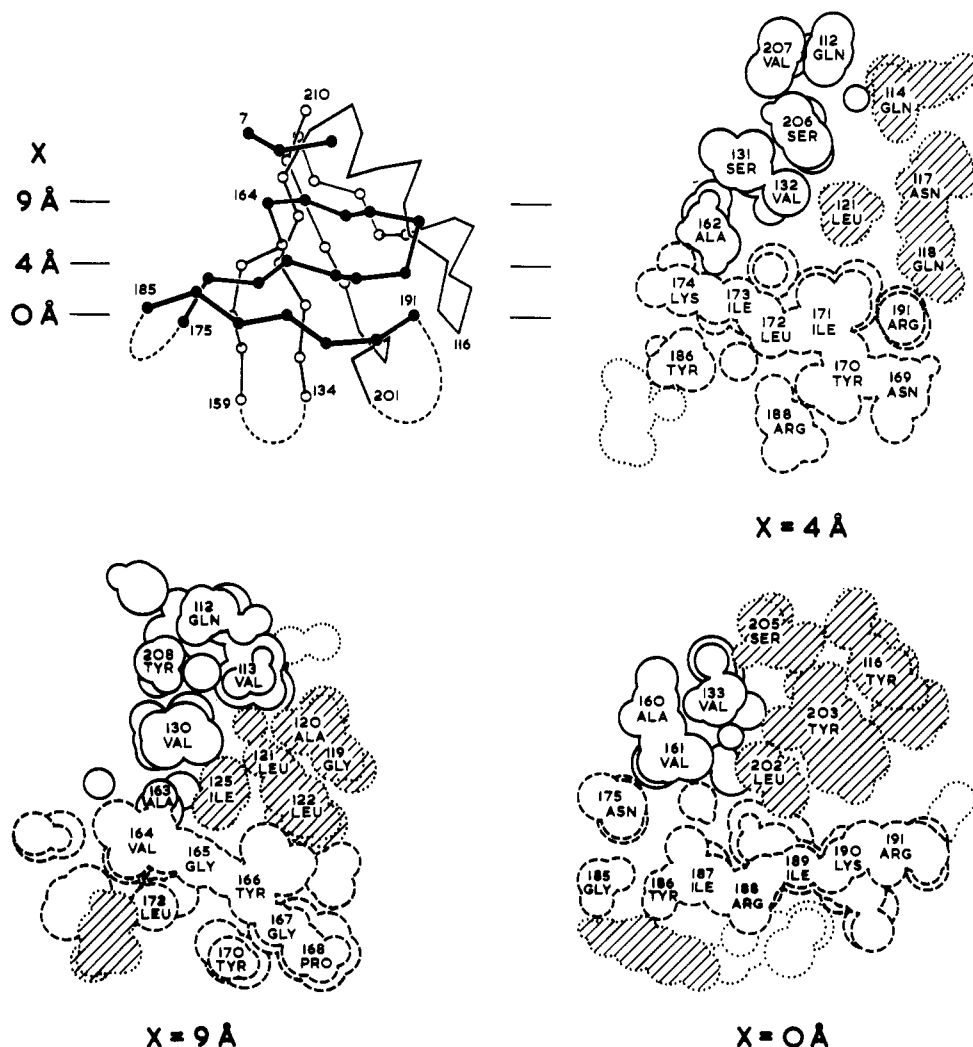


FIGURE 11: Residue packing in domain 2 of papain. See the legend to Figure 8 for a description of the convention used here. The strands of the near  $\beta$  sheet (broken lines) are in the plane of the page, and those of the far  $\beta$  sheet (solid lines) are perpendicular. Strands 108–113 and 130–134 of the far  $\beta$  sheet are connected by an  $\alpha$  helix, 117–128, that is sandwiched between the two  $\beta$  sheets.

as can be seen in Figure 11, where all three sections show the two  $\beta$  sheets at a large angle. They form a wedge-shaped cavity, which is occupied by an  $\alpha$  helix (117–128) that connects the first and third strands of the far  $\beta$  sheet, and by residues from the connecting loop 192–205.

**Amino Acid Composition of the  $\beta$ -Sheet to  $\beta$ -Sheet Contact Residues.** The  $\beta$  sheets in Figure 5 contain a total of 232 residues. Their amino acid composition, given in Table III, is not significantly different from that of a large sample of  $\beta$ -sheet residues in a variety of protein structures analyzed by Levitt (1978).

In elastase, alcohol dehydrogenase, and staphylococcal nuclease, 25% of the  $\beta$ -sheet residues are involved in the internal  $\beta$ -sheet to  $\beta$ -sheet packing. The proportion is somewhat higher in penicillopepsin (37%), where both faces of the middle  $\beta$  sheet make contacts, while in other proteins, only one face of each  $\beta$  sheet is involved in the packing. The amino acid composition of the contacts is very different from the average (Table III): of the 59 contact residues, 36, or 61%, are Val, Ile, or Leu. These residues account for only 27% of an average  $\beta$  sheet and for 33% of the residues buried inside an average protein (Janin, 1979). The preference for Val, Ile, or Leu in  $\beta$ -sheet interfaces is highly significant in orthogonal packings described here, in aligned  $\beta$ -sheet packings, where they form 48% of the contact residues (Chothia & Janin, 1981), and in  $\alpha$ -helix to  $\beta$ -sheet packings, where Val, Ile, and Leu account

for 49% of the  $\beta$ -sheet residues forming helix contacts (Janin & Chothia, 1980). Though the contacts in these interfaces have different geometries, the requirement for the larger hydrophobic residues is the same. The branched side chains of Val, Ile, and Leu contribute to form a smooth, well-packed surface on the  $\beta$  sheets.

The special amino acid composition of the contact residues affects the total composition of the  $\beta$  sheets. The effect is more important in  $\alpha/\beta$  proteins, where 67% of the  $\beta$ -sheet residues form helix contacts, than in aligned  $\beta$ -sheet packing, where only 33% of the residues form  $\beta$ -sheet to  $\beta$ -sheet contacts, or orthogonal  $\beta$ -sheet packing, where the fraction is even less. As a consequence, parallel  $\beta$  sheets, mostly found in  $\alpha/\beta$  proteins, and antiparallel  $\beta$  sheets, mostly found in all- $\beta$  proteins, differ in their acid composition (Lifson & Sander, 1979).

## Discussion

**Orthogonal  $\beta$ -Sheet Packing.** The main features of our model for orthogonal  $\beta$ -sheet packing are observed in the five proteins studied here. They contain six pairs (two in penicillopepsin) of  $\beta$  sheets that pack together with their strand directions orthogonal. At the ends of one diagonal, strands go from the top to the bottom  $\beta$  sheets to form close corners. At the ends of the other diagonal, the  $\beta$  sheets splay apart. In elastase, staphylococcal nuclease, alcohol dehydrogenase,

Table III: Amino Acid Composition of the  $\beta$  Sheets and Their Contact Residues<sup>a</sup>

residue	% amino acid composition		
	av $\beta$ sheet (a)	our sample of $\beta$ sheets (b)	contact residues in our $\beta$ sheets (c)
Val	11.9	16	31
Leu	7.0	9	17
Ile	7.8	9	14
Phe	4.6	2	7
Ala	7.6	8	5
Asp	4.3	5	5
Gly	8.7	6	3
Tyr	4.8	5	3
Trp	1.7	2	3
Thr	7.7	6	2
Glu	3.8	4	2
Asn	3.3	3	2
His	2.6	2	2
Gln	2.5	5	2
Pro	2.5	2	2
Met	1.5	2	2
Ser	7.6	6	0
Lys	5.4	5	0
Arg	3.0	4	0
Cys	1.6	0	0
total	99.9	101	102

<sup>a</sup> Amino acid compositions are calculated for (a) the 1555 residues representing an average  $\beta$  sheet (Levitt, 1978), (b) the 232 residues in the  $\beta$  sheets shown in Figure 5, and (c) the 58 residues marked there as forming  $\beta$ -sheet to  $\beta$ -sheet contacts.

and one of the penicillopepsin packings, the  $\beta$  sheets join at two diagonally opposite corners as in the model. In the other penicillopepsin packing and in papain, the  $\beta$  sheets are joined at only one corner.

Strands joining the  $\beta$  sheets are bent at the point where they form close corners. There are 13 such strands in our sample: 7 close corners involve 1  $\beta$  strand each and 3 other corners involve 2 adjacent  $\beta$  strands. We find a classic  $\beta$  bulge in 5 of the 13  $\beta$  strands, a  $\beta$  bend in another 6, and a short (two-residue) helical junction in 2. They all form right-handed 90° bends.

In orthogonal  $\beta$ -sheet packing, contacts between the  $\beta$  sheets are restricted to the diagonal joining close corners. Yet, they are similar to those in aligned  $\beta$ -sheet packings and to the  $\alpha$ -helix to  $\beta$ -sheet contacts in  $\alpha/\beta$  proteins in that they involve the smooth hydrophobic surfaces formed by side chains of Val, Ile, and Leu residues. In orthogonal  $\beta$  packings, the  $\beta$  sheets are also in contact with non- $\beta$ -sheet parts of the protein structure at splayed corners. In five cases, the contact is with an  $\alpha$  helix.

**Aligned  $\beta$ -Sheet Packing.** In the introduction, we noted that  $\beta$ -sheet packings can be divided into two classes. We have discussed the class where the strand directions of the different  $\beta$  sheets are at  $\sim 90^\circ$ ; in the other class, which we call aligned packings, they are inclined at  $\sim 30^\circ$  (Figure 1).

The immunoglobulin domains were the first examples of aligned  $\beta$ -sheet packing, later found in prealbumin, conalbumin A, superoxide dismutase, the blue copper proteins plastocyanin and azurin, two plant virus coat proteins, and  $\gamma$ -crystallin (Chothia & Janin, 1981). In these proteins, the interface residues of one  $\beta$  sheet are approximately aligned with the interface residues of the second  $\beta$  sheet. Because the  $\beta$  strands are twisted, this alignment of *side chains* puts the *main chains* of the two  $\beta$  sheets at an angle of  $\sim 30^\circ$ . This allows the  $\beta$  sheets to maintain a large contact area in spite of their twist. Cohen et al. (1981) have described the char-

acteristic arrangement of the contact residues in the  $\beta$  sheets.

We have used the most noticeable difference between orthogonal and aligned packings—the relative orientation of their  $\beta$  sheets—to define the two classes. However, they have other characteristic differences that are related to the two different modes of  $\beta$ -sheet association. At the close corners of orthogonal packings, the  $\beta$  sheets fuse and  $\beta$  strands cross from one layer to the other while bending by some 90°, yet they make normal H bonds to neighboring  $\beta$  strands. In contrast, aligned packings involve distinct  $\beta$  sheets, with the top and bottom connected through stretches of several residues in non- $\beta$  conformations, and with reversal of the polypeptide chain direction.

**Packed  $\beta$  Sheets and  $\beta$  Barrels.** The protein structures which we consider to be pairs of  $\beta$  sheets packed face to face are often described as barrels, or cylinders made of a single  $\beta$  sheet wrapped around (Birktoft & Blow, 1972; Richardson, 1977, 1981). In orthogonal  $\beta$ -sheet packings, some of the features of our model are similar to the  $\beta$ -barrel description: the H-bond pattern extends from one layer to the other and closes on itself. However, in our model, the curvature of the  $\beta$  sheets is not evenly distributed but principally located in the edge strands where anomalies such as  $\beta$  bulges or  $\beta$  bends play a peculiar role. In aligned  $\beta$ -sheet packings, H bonds between strands in the top and bottom  $\beta$  sheets are rare, not the rule. The actual shape of the structure is not a cylinder, but a twisted prism (Chothia & Janin, 1981).

A  $\beta$  barrel cannot be readily formed by the uniform distortion of a regular  $\beta$  sheet. From model building studies, Salemme and Weatherford found that the closure of coiled  $\beta$  sheets required localized irregularities (Weatherford & Salemme, 1981; Salemme, 1981). A cylinder made from a  $\beta$  sheet would have a diameter of 14 Å or more (McLachlan, 1979). In proteins, the close-packed  $\beta$  sheets are less thick: in aligned packings, the two layers are separated by 8.3–10.3 Å (Cohen et al., 1981); in orthogonal packings, the separation is 8.7–11.5 Å, for the proteins described here. In addition, the  $\Omega$  angle between strands on two sides of a  $\beta$  barrel should decrease when the number of  $\beta$  strands increases (Richardson, 1981). This is not what we find:  $\Omega$  is close to either  $-30^\circ$  or  $90^\circ$  irrespective of the number of strands.

## Conclusion

The rules that govern aligned and orthogonal  $\beta$ -sheet packings reflect properties of  $\beta$  sheets that are not directly dependent on their particular amino acid sequence. Within a class of packing, the sequence affects the details of  $\beta$ -sheet interfaces, but not their general geometry. We have drawn the same conclusion from our studies of helix to helix and helix to  $\beta$ -sheet packings. Taken together, these studies show how geometric constraints may impose similar folds on unrelated sequences, as often occurs in proteins of the same structural class.

## Acknowledgments

We are grateful to J. Cresswell for the illustrations, M. Levitt and D. Richardson for computer programs, and A. Jones and C. Bränden for the atomic coordinates of alcohol dehydrogenase.

## References

- Arnone, A., Bier, C. J., Cotton, F. A., Day, V. W., Hazen, E. E., Jr., Richardson, D. C., Richardson, J. S., & Yonath, A. (1971) *J. Biol. Chem.* 246, 2302–2316.
- Birktoft, J., & Blow, D. M. (1972) *J. Mol. Biol.* 68, 187–240.

- Chothia, C. (1973) *J. Mol. Biol.* 75, 295-302.
- Chothia, C., & Janin, J. (1981) *Proc. Natl. Acad. Sci. U.S.A.* 78, 4146-4150.
- Chothia, C., Levitt, M., & Richardson, D. C. (1977) *Proc. Natl. Acad. Sci. U.S.A.* 74, 4130-4134.
- Chothia, C., Levitt, M., & Richardson, D. C. (1981) *J. Mol. Biol.* 145, 215-250.
- Cohen, F. E., Sternberg, M. J. E., & Taylor, W. R. (1980) *Nature (London)* 285, 378-382.
- Cohen, F. E., Sternberg, M. J. E., & Taylor, W. R. (1981) *J. Mol. Biol.* 148, 253-272.
- Crick, F. H. C. (1953) *Acta Crystallogr.* 6, 689-691.
- Drenth, J., Jansonius, J. N., Koekoek, R., & Wolthers, B. G. (1971) *Adv. Protein Chem.* 25, 79-115.
- Efimov, A. V. (1977) *Dokl. Akad. Nauk SSSR* 235, 699-702.
- Efimov, A. V. (1979) *J. Mol. Biol.* 134, 23-40.
- Eklund, H., Nordström, B., Zeppezauer, E., Soderlund, G., Ohlsson, I., Boive, T., Sodeberg, B. O., Tapia, O., Brändén, C. I., & Akeson, A. (1976) *J. Mol. Biol.* 102, 27-59.
- Hsu, I. N., Delbaere, L. T. J., James, M. N. G., & Hoffman, T. (1977) *Nature (London)* 266, 140-145.
- Janin, J. (1979) *Nature (London)* 277, 491-492.
- Janin, J., & Chothia, C. (1980) *J. Mol. Biol.* 143, 95-128.
- Levitt, M. (1978) *Biochemistry* 17, 4277-4284.
- Lifson, S., & Sander, C. (1979) *Nature (London)* 282, 109-110.
- McLachlan, A. D. (1979) *J. Mol. Biol.* 128, 49-79.
- Richardson, J. S. (1977) *Nature (London)* 268, 495-500.
- Richardson, J. S. (1981) *Adv. Protein Chem.* 34, 168-339.
- Richardson, J. S., Getzoff, E. D., & Richardson, D. C. (1978) *Proc. Natl. Acad. Sci. U.S.A.* 75, 2574-2578.
- Richmond, T. J., & Richards, F. M. (1978) *J. Mol. Biol.* 119, 537-555.
- Salemme, F. R. (1981) *J. Mol. Biol.* 146, 143-156.
- Sawyer, L., Shotton, D. M., Campbell, J. W., Wendell, P. L., Muirhead, H., Watson, H. C., Diamond, R., & Ladner, R. C. (1978) *J. Mol. Biol.* 118, 137-208.
- Venkatachalam, C. M. (1968) *Biopolymers* 6, 1425-1436.
- Weatherford, D. W., & Salemme, F. R. (1979) *Proc. Natl. Acad. Sci. U.S.A.* 76, 19-23.
- Weatherford, D. W., & Salemme, F. R. (1981) *J. Mol. Biol.* 141, 101-117.

## Resolution of Multiple Heme Centers of Hydroxylamine Oxidoreductase from *Nitrosomonas*. 1. Electron Paramagnetic Resonance Spectroscopy<sup>†</sup>

John D. Lipscomb and Alan B. Hooper\*

**ABSTRACT:** Hydroxylamine oxidoreductase (HAO) from *Nitrosomonas europaea* [ $M_r$  220 000, subunit structure of  $(\alpha\beta)_3$  with seven *c*-type hemes and one P-460-type heme per  $\alpha\beta$  subunit] catalyzes the oxidative conversion of  $\text{NH}_2\text{OH}$  to  $\text{NO}_2^-$ . We have used electron paramagnetic resonance (EPR) spectroscopy to monitor a reductive titration of the enzyme. The spectra show that the *c*-type hemes can be placed into at least four groups with different oxidation-reduction potentials and protein environments. Since the hemes are reduced sequentially, *g*-value assignments can be made for three of the major species ( $g = 3.38, 1.95, 0.7$ ;  $g = 3.06, 2.14, 1.35$ ; and  $g = 2.98, 2.24, 1.44$ ), and the spectrum of each can be isolated from the composite spectrum of the protein. Quantitation of these three spectra suggests that approximately one-third of the heme in the enzyme resides in other species. Some of the unquantitated heme may contribute to one or more novel EPR active species with *g* values at  $g = 2.7$ ,  $g = 1.85$ , and  $g = 1.66$ .

A second fraction of this heme is probably EPR silent since high- and low-spin heme signals absent from the spectrum of resting HAO appear during the final half of the reductive titration. One of these newly EPR active species, with characteristic high-spin heme *g* values at 6.45 and 5.6, reduces concomitantly with the appearance of the optical spectrum of the reduced P-460 heme. On this basis, P-460 is tentatively assigned as the high-spin heme. Since no high-spin heme signal is observed in the resting enzyme, P-460 must either undergo a spin conversion as the other hemes are reduced or be EPR silent due to spin coupling or fast electronic spin relaxation. EPR spectra also show that  $\text{NH}_2\text{OH}$  reduces approximately 45% of the hemes when complexed anaerobically with HAO. A new low-spin heme ( $g = 2.86, 2.3$ ) becomes EPR active in this complex, and the *g* values of most of the other EPR active hemes shift slightly.

Ammonia in aerobic soils or waters is rapidly oxidized to nitrite as the sole source of energy by the autotrophic nitrifying bacterium *Nitrosomonas europaea*. Hydroxylamine, or a closely related enzyme-bound chemical species, is an intermediate in the process (Hooper, 1978). The enzyme hy-

droxylamine oxidoreductase (HAO)<sup>1</sup> isolated from the bacterium catalyzes the rapid aerobic oxidation of hydroxylamine to nitrite in the presence of phenazine methosulfate as an artificial electron acceptor. HAO ( $M_r$  220 000) has been shown to contain approximately 21 *c*-type hemes and 3 residues of an unusual prosthetic group termed P-460 (Hooper et al., 1978). The active enzyme is composed of three  $M_r$  11 000  $\alpha$  subunits each containing one *c*-type heme and three  $M_r$  63 000  $\beta$  subunits each containing approximately six *c*-type hemes as well as the P-460 (Terry et al., 1979; Terry & Hooper, 1981). No evidence for the presence of other essential metal centers

<sup>†</sup> From the Department of Biochemistry, Medical School, University of Minnesota, Minneapolis, Minnesota 55455 (J.D.L.), and the Department of Genetics and Cell Biology, University of Minnesota, St. Paul, Minnesota 55108 (A.B.H.). Received October 26, 1981; revised manuscript received April 14, 1982. This research was supported by the National Science Foundation through Grant PCM 8008710 (to A.B.H.) and by the National Institutes of Health through Grant GM 24689 (to J.D.L.). The EPR spectrometer at the University of Minnesota was purchased in part through grants from the Minnesota Medical Foundation and the Graduate School.

<sup>1</sup> Abbreviations: EPR, electron paramagnetic resonance; HAO, hydroxylamine oxidoreductase; EDTA, ethylenediaminetetraacetic acid.